Environmental Science & Technology

pubs.acs.org/est

Article

Linking Increased Isotope Fractionation at Low Concentrations to Enzyme Activity Regulation: 4-Cl Phenol Degradation by *Arthrobacter chlorophenolicus* A6

Kankana Kundu,* Aileen Melsbach, Benjamin Heckel, Sarah Schneidemann, Dheeraj Kanapathi, Sviatlana Marozava, Juliane Merl-Pham, and Martin Elsner*

Cite This: *Environ. Sci. Technol.* 2022, 56, 3021−3032

Read Online

ACCESS | Metrics & More | Article Recommendations | Supporting Information

ABSTRACT: Slow microbial degradation of organic trace chemicals ("micropollutants") has been attributed to either downregulation of enzymatic turnover or rate-limiting substrate supply at low concentrations. In previous biodegradation studies, a drastic decrease in isotope fractionation of atrazine revealed a transition from rate-limiting enzyme turnover to membrane permeation as a bottleneck when concentrations fell below the Monod constant of microbial growth. With degradation of the pollutant 4-chlorophenol (4-CP) by *Arthrobacter chlorophenolicus* A6, this study targeted a bacterium which adapts its enzyme activity to concentrations. Unlike with atrazine degradation, isotope fractionation of 4-CP *in*creased at lower concentrations, from $\varepsilon(C) = -1.0 \pm 0.5‰$ in chemostats ($D = 0.090\ h^{-1}$, 88 mg L^{-1}) and $\varepsilon(C) = -2.1 \pm 0.5‰$ in batch (c_0 = 220 mg L^{-1}) to $\varepsilon(C) = -4.1 \pm 0.2‰$ in chemostats at 90 μg L^{-1}. Surprisingly, fatty acid composition indicated increased cell wall permeability at high concentrations, while proteomics revealed that catabolic enzymes (CphCI and CphCII) were differentially expressed at $D = 0.090\ h^{-1}$. These observations support regulation on the enzyme activity level—through either a metabolic shift between catabolic pathways or decreased enzymatic turnover at low concentrations—and, hence, reveal an alternative end-member scenario for bacterial adaptation at low concentrations. Including more degrader strains into this multidisciplinary analytical approach offers the perspective to build a knowledge base on bottlenecks of bioremediation at low concentrations that considers bacterial adaptation.

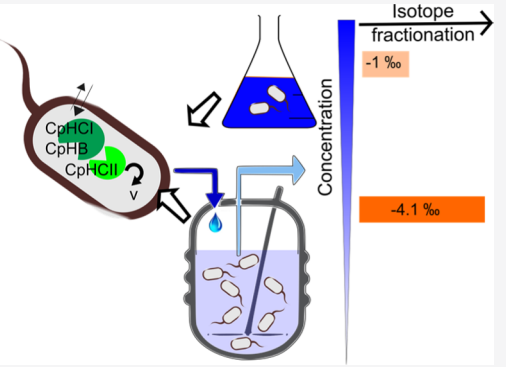

KEYWORDS: *limits of biodegradation, mass transfer, enzyme regulation, cell wall permeability, chemostat, proteomics, isotope effect*

INTRODUCTION

Organic contaminants such as pesticides, personal care products, steroid hormones, and pharmaceuticals are frequently detected in the aquatic environment at low concentrations (ng L^{-1} to μg L^{-1})[1,2] These low-level contaminants—referred to as chemical micropollutants—bear potential to impact ecosystems[3] so that their natural degradation is of great relevance. Many of these pollutants were found to be biodegradable in studies at high concentrations, at which degrading organisms could be cultivated and isolated from contaminated environments.[4−6] Nonetheless, the increasingly frequent detection of micropollutants in aquatic environments indicates that their turnover must be very slow to nonexistent at low environmental concentrations.[7,8] This observation is mirrored by the persistence of assimilable organic carbon (AOC) in aquatic environments on the order of 1−100 μg L^{-1} where concentrations of individual sugars are only a few μg L^{-1}. This suggests that contaminants and degradable biomolecules alike may become "persistent by dilution".[9] Despite such slow degradation of AOC and despite an energy-limited environment, where microorganisms face continuous exposure to low concentrations, viable cell counts still amount to 10^5 to 10^6 cells mL^{-1},[9−11] of which most (∼70%) maintain their activity.[12,13] Hence, understanding activity, intrinsic limitations, and microbial adaptation to low concentrations is important, not only to understand the physiology of microorganisms under extreme environmental conditions but also for micropollutant management and remediation strategies when compounds are in principle biodegradable and organisms are active, but degradation is inexplicably slow.

Two competing paradigms may rationalize such a low activity at low concentrations. First, uptake of micropollutants

Received: July 23, 2021
Revised: January 23, 2022
Accepted: January 26, 2022
Published: February 11, 2022

into microbial cells (active/passive transport) may become rate-limiting when the enzyme reaction shifts from zero- to first-order kinetics at low concentrations so that intracellular substrate levels are drained.[14−16] Alternatively, enzymatic turnover may become rate-limiting when microorganisms adapt their physiology to low concentrations—for example, by switching to maintenance mode and downregulating catabolic enzymes[17,18]—so that enzymatic degradation slows or even stalls below a particular low concentration. With conventional methods, it is challenging to identify the bottleneck—mass transfer or enzyme activity—under these circumstances. Insights from compound-specific isotope analysis (CSIA) offer complementary evidence. CSIA measures the ratios of stable isotopes at their natural abundance in a compound. The isotope effect of enzymatic reactions usually discriminates against heavy isotopes and, therefore, leads to an enrichment of heavy relative to light isotopes in the remaining pollutant molecules next to the enzyme.[19] If this enrichment can also be observed outside the cell in solution, it makes CSIA a unique approach to determine turnover of micropollutants in natural systems. Such an isotope fractionation is typically observed in microbial degradation at high concentrations when enzymes inside the cell are substrate-saturated and enzymatic turnover runs at zero-order kinetics (V_{max}). Under these conditions, mass transfer across the cell membrane is fast in comparison, and intra- and extracellular substrate concentrations are in rapid equilibrium.[20,21] At low concentrations—depending upon microbial adaptation—however, two scenarios can arise: one where the enzyme reaction remains the rate-determining step and the other where mass transfer into the cell becomes limiting.[21] In analogy to insights from isotope fractionation of CO_2 in photosynthesis of C_3 versus C_4 plants[22] or in algae when uptake becomes limiting,[23,24] here, observable isotope fractionation can provide conclusive evidence. (i) If intracellular concentrations fall below the Michaelis Menten constant, enzymatic turnover will no longer run at saturation but follow first-order kinetics. The enzyme reaction may consequently become fast relative to mass transfer into and out of the cell so that cell membrane passage becomes the bottleneck of the overall transformation (Scenario 1 above). In such a situation, the isotope effect—which still occurs next to the enzyme—will no longer be represented outside the cell because molecules are quicker to be converted than to diffuse out and make the isotope discrimination visible in solution. Hence, concomitant to mass transfer limitations, the isotope fractionation that is experimentally observed outside the cell will become masked and decrease.[15,16,25] (ii) In contrast, if the enzymatic turnover remains slower than the mass transfer across the cell membrane—corresponding to scenario 2 mentioned above—the opposite trend will be observed: isotope fractionation will be fully expressed, similarly as at high concentrations.

In degradation of the prevalent micropollutant atrazine with *Arthrobacter aurescens* TC1,[26] a drastic decrease in isotope fractionation revealed that scenario 1 prevailed: at about 60 $\mu g\ L^{-1}$, mass transfer through the cell membrane became limiting implying that the enzyme machinery remained fully active at low concentrations.[27,28] While intriguing, insights from this study are based on the response of only one microorganism cultivated with one specific micropollutant, and it represents a case where enzyme activity was not reported to respond to specific micropollutant concentrations. It is well-recognized that organisms exist (i) whose enzyme activity is regulated by the micropollutant concentration, either on the expression level of metabolic pathways (up/downregulation[9,18,29,30]) or directly on the level of enzyme activity (inhibition[31−33] and activation[34,35]), and, further, (ii) whose cell membrane may change in response to high versus low concentrations of a compound so that membrane permeability and, thus, mass transfer are also modulated.[36,37]

Phenolic compounds, for example, 4-chlorophenol (4-CP), represent a specific category of pollutants which are known for acute toxicity that has a regulating effect on both enzyme activity[38,39] and cell membrane fluidity so that mass transfer across the cell membrane is also modulated.[40] Attention has been paid to isolation of degrader strains and to the influence of high, toxic concentrations on growth kinetics.[5,41] In contrast, it remains to be investigated how degraders adapt to low concentrations and what influence changes in cell membrane fluidity, as well as enzyme activity regulation, have on limiting 4-CP turnover at low concentrations. Specifically, it was our objective to investigate whether concentrations may have a regulating effect on enzymatic turnover of 4-CP so that—unlike in the case of *A. aurescens* TC1—it would be enzymatic turnover rather than mass transfer through the cell membrane that becomes rate-limiting at low concentrations. To explore this, *Arthrobacter chlorophenolicus* A6 was chosen as a model microorganism which can degrade various phenolic compounds.[5] The availability of a fully sequenced genome,[42] experimental evidence of membrane adaptation at varying concentrations,[37] and the presence of inducible degradation enzymes that can catalyze two catabolic pathways simultaneously[42,43] make this organism a promising candidate to explore the effect of physiological adaption/regulation on the bottleneck of phenolic compound degradation at low concentrations. Previous studies targeted CSIA during biodegradation of phenolic compounds at high concentrations[44] or they explored the indirect influence of phenolic compounds on isotope fractionation of a different substrate—the electron acceptor nitrate.[45] Here, it was our aim to directly measure the observable isotope fractionation of 4-CP during ongoing degradation along with analysis of membrane fatty acids and the proteome state of the cells at varying concentrations. To investigate two end-member scenarios, *A. chlorophenolicus* A6 was cultivated at high concentrations (mg L^{-1}) in batch and chemostats and at low concentrations ($\mu g\ L^{-1}$) in chemostats. In both cases, observable isotope fractionation was measured to explore limitations by mass transfer. To probe for physiological adaptation, (i) flow cytometry was performed to inform about the fraction of viable to total cells, (ii) comparative label-free proteomics was conducted to observe changes in protein expression, and (iii) the cell membrane fatty acid composition was analyzed to test for changes in membrane fluidity.

MATERIALS AND METHODS

Cultivation in Batch and Chemostats. *A. chlorophenolicus* A6 (DSMZ, Germany) was grown on mineral salt (MS) medium supplemented with 220 (1.71 mM) mg L^{-1} 4-CP and 0.5 g L^{-1} (6.25 mM) NH_4NO_3 (Sigma-Aldrich, Germany) as a source of C and N, respectively.[5] The medium was prepared in MilliQ water where the total organic carbon content was less than 10 $\mu g\ L^{-1}$ and the pH was adjusted to 7.2 with sodium hydroxide (1.0 M). The medium was autoclaved at 121 °C for 20 min and cooled. After autoclaving, the media was spiked with 4-CP (≥99%, 1.3 g mL^{-1}, Sigma-Aldrich, Germany) and

https://doi.org/10.1021/acs.est.1c04939
Environ. Sci. Technol. 2022, 56, 3021−3032

NH_4NO_3 (stock solution = 20 g L^{-1} and filter-sterilized) to reach a final concentration of 220 mg L^{-1} and 0.5 g L^{-1}, respectively. This was followed by the addition of a filter-sterilized $FeCl_3 \cdot 6H_2O$ solution (5.14 mg L^{-1}). To prepare a preculture for subsequent batch and chemostat (continuous cultivation) degradation experiments, *A. chlorophenolicus* A6 was grown on MS media with 4-CP and NH_4NO_3 in a shaken flask at 300 rpm until an optical density at 600 nm (OD_{600}) of 0.15 (mid-exponential phase) was reached. For batch degradation experiments, cells were harvested by centrifuging 50 mL of preculture, washing the pellet twice in sterile MS media, and resuspending it in 1 mL of sterile MS media. This suspension was added to 500 mL of MS media supplemented with 220 mg L^{-1} 4-CP to initiate the degradation of 4-CP at 25 °C. Subsequently, samples were taken for concentration and isotope analysis of 4-CP and cell concentration measurements over time and data were used to estimate Haldane inhibition kinetic constants (see the Supporting Information).

The continuous cultivation of *A. chlorophenolicus* A6 was performed in custom-made bioreactors equipped with a magnetic stirrer, where the agitation speed was maintained at 300 rpm (Supporting Information, Figure S1). In such chemostats, the growth of microorganisms is determined by the rate of in- and outflow, where wash-out of media and microorganisms is balanced by continuous addition of media and growth of bacteria. At high flow/dilution rates D [defined as the ratio of the medium flow rate (mL h^{-1}) and cultivation volume (L)], the reactor volume is quickly exchanged so that bacteria grow more quickly to maintain a steady-state cell concentration. At low D, in contrast, growth rates become small. Periodic aeration of the culture was achieved by pumping air through an L-shaped tube sparger assembly. Specifically, an intermittent flow of air at a rate of 0.03 L-air L^{-1} min^{-1} was sparged to maintain the oxygen saturation level in the range of 40−70% as monitored using a pO_2 probe (Applikon Biotechnologie B.V., Netherlands). No loss of 4-CP was observed. The feeding bottle was tightly closed and connected to another bottle with the same concentration of 4-CP solution to exclude substance loss by evaporation into the gas phase in the feeding reservoir. The working volume of the bioreactor was maintained at 1600 mL, the pH was held constant at 7.2, and the temperature was 25 °C. A preculture of *A. chlorophenolicus* A6 [10% (v/v)] was used for inoculation. The bioreactors were operated at three dilution rates (D) of 0.018, 0.038, and 0.090 h^{-1} corresponding to a hydraulic retention time (HRT) of 3, 1, and 0.46 days, respectively. Dilution rates were only changed after achieving a steady state at a particular D. The steady state was defined by constant cell densities and 4-CP concentrations (<5 and <10% relative variation, respectively) for at least four HRTs. All cultivations were performed in duplicates. Due to the toxicity of 4-CP and intermediates of its catabolic breakdown,[43] the cultivation vessels were kept in the safety hood; also, to exclude photodegradation, they were protected from light (covered by aluminum foil).

Measurement of Substrate (4-CP) Concentrations and Biomass. Samples were taken at different time points during batch degradation and continuous operation of the bioreactors. After filtering the samples, concentration measurements of 4-CP were conducted using a Prominence HPLC system (Shimadzu Corp., Japan) equipped with a 150 × 4.6 mm Ultracarb 5 μm ODS (30) 60 Å column (Phenomenex Inc., USA) and UV detector. Details of the HPLC method are provided in the Supporting Information. To measure the cell dry weight, samples from chemostats at the steady state were centrifuged at 4 °C in a preweighed tube washed with 0.9% NaCl and dried at 85 °C to constant weight.[30]

Determination of Cell Numbers, Viability, and Morphology. Cells were stained with SYBR Green I and propidium iodide to estimate the number of total cells and viable cells by flow cytometry, respectively, as described in Kundu et al.[27] The cell concentration measurements were used to define the steady state in the chemostats and for calculating the specific growth rate[46] in batch cultivation. For morphology, the cells were analyzed on agar glass slides by light microscopy with an Axioscope 2 Plus microscope (Carl Zeiss AG, Germany).[47]

Consumption Rate of 4-CP. The specific substrate consumption rate of 4-CP was represented as q_s, that is, the quotient of substrate consumption rate per hour and biomass present in the vessel (mg S mg C_x h^{-1}). q_s was calculated as

$$q_s = \frac{\mu}{Y_{opt}} \tag{1}$$

where μ is the specific growth rate (in chemostats at steady state, $\mu = D$) and Y_{opt} is the operational yield, that is, mg biomass produced per mg of the substrate consumed where biomass was determined from cell dry weight experimentally as described above. In chemostats, Y_{opt} was determined as described below

$$Y_{opt} = \frac{X}{S_0 - S} \tag{2}$$

where X is biomass concentration measured at the steady state, S_0 is the 4-CP concentration in the medium, and S is the residual 4-CP concentration at the steady state.

Gas Chromatography Isotope Ratio Mass Spectrometry Analysis of 4-CP Samples in Batch and Chemostats. Carbon isotope values of the 4-CP (Sigma-Aldrich, Germany) used in the cultivation were determined beforehand using an elemental analyzer coupled with isotope ratio mass spectrometry (EA-IRMS). Details of the method are included in the Supporting Information. For isotope analysis, 10−20 mL of sample volume was withdrawn from batch and 100−200 mL from chemostats at the steady state. Samples were filtered within 5 min (pore size 0.2 μm, diameter 47 mm; GE Healthcare Ltd., UK) to stop degradation. Degradation during this time was verified to be less than 1% (data not shown). After filtration, 4-CP was extracted with dichloromethane (DCM, 5% of the sample volume, three times, resulting in an overall extraction efficiency of app. 90% and no changes in isotope values). DCM was partly evaporated (not to complete dryness) at room temperature using a gentle nitrogen stream, and finally, 4-CP was reconstituted in 100 μL of DCM. Simultaneously, 1 mL of the medium which was fed to the chemostats was collected, frozen at −80 °C, and dried by lyophilization, and 4-CP was reconstituted in 100 μL of DCM. Controls ensured the absence of isotope fractionation during these operations. Carbon isotope analysis of 4-CP was performed on a gas chromatography-IRMS (GC-IRMS) system (Thermo Fisher Scientific, Waltham, Massachusetts, USA) consisting of a Trace GC with a PAL autosampler (CTC Analytics) equipped with a DB-5 analytical column (30/60 m, 0.25 mm ID, 0.25/1 μm film, Agilent Technologies, Germany) coupled to a Finnigan MAT 253 isotope ratio mass

https://doi.org/10.1021/acs.est.1c04939
Environ. Sci. Technol. 2022, 56, 3021−3032

spectrometer via a Finnigan GC Combustion III interface (both Thermo Fisher Scientific, Germany).

Values of $\delta^{13}C$ of 4-CP in per mil (‰) are reported relative to PeeDee Belemnite (V-PDB) using the following equation[49]

$$\frac{(R)_x}{(R)_{ref}} - 1 = \frac{\left(\frac{^{13}C}{^{12}C}\right)_x}{\left(\frac{^{13}C}{^{12}C}\right)_{ref}} - 1 = \delta^{13}C \quad (3)$$

where R is the ratio of heavy (^{13}C) and light (^{12}C) carbon isotopes, respectively, in a sample (x) and reference (ref). Determination of $\delta^{13}C$ values was performed relative to the laboratory CO_2 monitoring gas, which was introduced at the beginning and the end of each analysis run. The laboratory CO_2 was calibrated to the international reference material VPDB by the reference CO_2 standard (RM8563) supplied by the International Atomic Energy Agency. The enrichment factor (ε) for batch degradation was calculated using the classic Rayleigh equation[48,49]

$$\ln \frac{R_t}{R_0} = \frac{\delta^{13}C + 1}{\delta^{13}C_0 + 1} = \varepsilon \cdot \ln f \quad (4)$$

where R_t and R_0 are compound-specific isotope ratios of heavy versus light isotopes at a given time and at the beginning of the reaction, respectively, and f is the fraction of the remaining pollutant in the time course of reaction or degradation. In the case of samples from chemostat experiments where 4-CP was continuously added and the outflow was withdrawn, ε was calculated as per the following equation[28]

$$\varepsilon = (\delta^{13}C_{in} - \delta^{13}C_{chemostat})/(1 - f) \quad (5)$$

where δ_{in} and $\delta_{chemostat}$ refer to carbon isotope ratios of 4-CP in inflow and outflow of the chemostat, respectively, and $f = (conc_{chemostat}/conc_{in})$ denotes the fraction of the residual substrate in the chemostat (eq 2.23 in Hayes, 1983[50]). Samples from each sampling event were split into 3−6 technical replicates for isotope measurements. Even though concentrations in the outflow of chemostats were as low as 90 μg/L, our sampling protocol ensured sufficient mass (1500 ppm in the extracts, 1 nmol on-column) for peak amplitudes of 2 V ensuring precise isotope analysis (see Figure S9). Overall analytical uncertainty, 2σ of carbon isotope measurements, was ±0.5‰. For evaluating isotope ratios of samples from batch experiments, measurements were bracketed by laboratory standards so that the principle of identical treatment by Werner and Brand[51] could be applied where isotope values are determined against those of precharacterized standards and values are expressed as arithmetic means of 3−6 replicate measurements with their respective standard deviations (±σ). For analysis of samples from chemostat experiments, samples from in- and outflow were measured intermittently so that the enrichment factor for each biological replicate at each dilution rate could be determined as described above (eq 5) from six technical replicates without additional calibration by external standards. These technical replicates did not differ significantly from one another at the 0.05 level for each dilution rate. Hence, the enrichment factors of the two biological replicates were combined and the average is reported.

Lipid Extraction and Membrane Fatty Acid Analysis. To extract membrane lipids and generate fatty acid methyl esters (FAMEs), the "Sherlock Microbial Identification System" was used.[52] A sample volume of 2 mL was used for extraction and analysis. In brief, the fatty acids were separated from the rest of the lipid by saponification followed by methylation and extraction. The FAMEs were analyzed using a gas chromatograph coupled to a mass spectrometer (GC−MS) equipped with a split/splitless injector (FinniganTrace Ultra and Trace DSQ, Thermo Electron Corporation, Waltham, MA, USA) on a CP-Sil 88 capillary column (Agilent Technologies, Netherlands; 50 m × 0.25 mm × 0.20 μm film). The fatty acids were identified by their retention time and mass spectrum in comparison with an authentic standard mix containing different FAMEs (EURISO-TOP GmbH, Saarbrücken, Germany). The ratio of anteiso-pentadecanoic acid (anteiso-C15:0) to iso-pentadecanoic acid (iso-C15:0) was calculated as follows

$$\frac{\text{anteiso}}{\text{iso}}\ \text{ratio} = \frac{\text{Area(C15: 0 anteiso)}}{\text{Area(C15: 0 iso)}} \quad (6)$$

Details of the method are provided in the Supporting Information.

Proteomics Analysis. For proteomics analysis, 200 mL of sample volume was withdrawn from chemostats at steady state and 20 mL from batch experiments. Details of protein extraction are reported in our previous publication.[27] Ten micrograms of the whole protein extract from each sample was used for trypsin digestion using a modified FASP procedure.[53] The details of label-free quantification are provided in the Supporting Information. Normalization of raw abundance data of all unique peptides allocated to each protein were performed using Progenesis QI software.

Analysis of normalized abundances of proteins detected under different cultivation conditions was carried out using the *limma* R/Bioconductor package.[54] A multidimensional scaling (MDS) plot based on log2-transformed protein abundances quantified for different conditions was generated to show the relationship between different samples. Analysis of differential protein abundances was performed using the Limma-Voom in Bioconductor pipeline.[54,55] The voomWithQualityWeights function was used, which determines both observation-level and sample-specific weights for subsequent linear modeling. After *voom* transformation, Empirical Bayes-moderated t-statistics were used to assess the differentially abundant proteins between different conditions.[56] The undetected proteins were handled in the same way as for linear models.[56] A cutoff in the log fold change (LFC) higher than log2(2.5) and a Benjamini−Hochberg[57]-corrected P-value of <0.05 were applied for the proteins to be differentially abundant during the pairwise comparison between different conditions. Normalized protein abundance of each protein was converted to z-score using the transformation $[x - \text{mean}]/\text{SD}$, where x is one protein in the data set population and SD is the standard deviation. Hierarchical clustering of the z-scores for the differentially abundant proteins and all quantified proteins was performed using "Euclidean distance" as a distance function and was visualized as heat maps with the seaborn package.[58]

RESULTS AND DISCUSSION

Chemostat Cultivation Revealed That Degradation Activity Was Downregulated at Low Concentrations. 4-CP was degraded in batch (S_0 = 220 mg L^{-1}) up to 82% within 55 h (Supporting Information, Figure S2). This confirms that *A. cholorophenolicus* can withstand high and toxic concen-

https://doi.org/10.1021/acs.est.1c04939
Environ. Sci. Technol. 2022, 56, 3021−3032

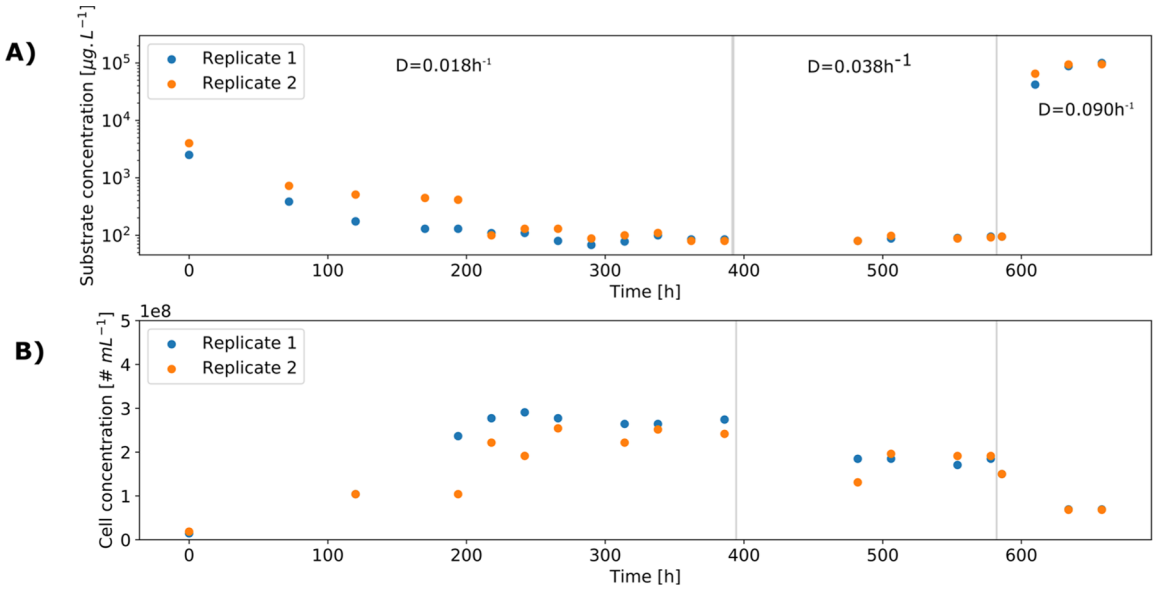

Figure 1. Chemostat cultivation reveals that degradation activity was regulated on the enzyme level. (A) Concentration of residual 4-CP at different dilution rates in chemostats. (B) Cell numbers per milliliter at different dilution rates.

trations of 4-CP as suggested by Westerberg et al.[5] In addition, 4-CP is known to be inhibitory to *A. chlorophenolicus* A6,[37] where substrate inhibition follows a fundamental biological regulatory mechanism.[59] The regulating effect has also been reported in the microbial growth rate which—in contrast to classical Monod growth kinetics—was found to become lower at high concentrations[60,61] and even the lag phase of the microbial growth curve was found to be extended at high inhibitory concentrations.[5,60] Analogous observations were made in this study and could be modeled by Haldane kinetics (see Figures S2 and S3).

After observing an expected regulating effect at high 4-CP concentrations (mg L^{-1} range) in batch experiments, we explored adaptation in the low-concentration regime in chemostat experiments (Figure 1A,B). The residual steady-state 4-CP concentration in chemostats operated at a D of 0.018 h^{-1} was 90 ± 10 μg L^{-1} or 0.7 ± 0.1 μM, which is much smaller than the Monod constant of K_s = 0.012 mM estimated from kinetic modeling (Supporting Information, Figure S3). The viable cell count at this concentration was ~2.22 ± 0.32 × 10^8 cells mL^{-1}. Remarkably, changing the D to 0.038 h^{-1} did not introduce significant changes in the 4-CP concentration (95 ± 10 μg L^{-1}) at the steady state (Figure 1A) neither was an apparent change in the biomass in terms of cell concentration (1.92 ± 0.32 × 10^8 cells mL^{-1}) observed (Figure 1B). This is in stark contrast to the classical behavior of chemostat experiments where residual substrate concentrations decrease with a decrease in D.[17] Previously, this kind of behavior was observed in benzoate degradation where no significant change in residual concentration was observed after changing D, an observation which was attributed to regulation of enzymatic turnover by altered degradation protein abundance.[18] Hence, the fact that the same residual concentration was observed even after doubling D implies that degradation activity at low concentrations of 4-CP must have been regulated leading to slower turnover and higher residual concentrations than expected—also in comparison with the batch degradation experiment, in which 4-CP was completely degraded (Supporting Information, Figure S2).

It was only at an extremely high dilution rate of D = 0.09 h^{-1} that steady-state cell concentrations decreased to 6.83 ± 0.12 × 10^7 cells mL^{-1} and a stark increase in 4-CP concentrations to 88 ± 8 mg L^{-1} (0.68 mM) was finally observed (Figure 1A,B). Since under these conditions, residual 4-CP concentrations (S) greatly exceeded the Haldane inhibition constant K_I = 12.0 mg L^{-1} from kinetic modeling (Supporting Information, Figure S3), this inhibitory effect is fully consistent with our observation of inhibition at high substrate concentrations from batch. Combined evidence from batch and chemostats therefore suggests that 4-CP degradation was not only inhibited at high 4-CP concentrations—as known from the literature[59] and modeled by Haldane kinetics (Supporting Information, Figure S3)—but we discovered that turnover was in addition decreased by regulation of enzyme activity at low concentrations. In a next step, we therefore explored whether such a regulation of enzyme activity was associated with changes in isotope fractionation.

Pronounced Isotope Fractionation in Chemostats Indicates That 4-CP Degradation Was Not Strongly Mass Transfer-Limited at Low (90 μg L^{-1}) Concentrations. In a batch experiment starting at high concentrations (c_0 = 220 mg L^{-1}), isotope analysis of 4-CP at different degradation time points showed significant changes in isotope values $^{13}C/^{12}C$ ($\delta^{13}C$) in the remaining 4-CP (Figure 2A). Determination of the carbon isotope enrichment factor according to the Rayleigh equation resulted in a value of ε = −2.1 ± 0.5‰. No isotope fractionation was observed in sterile controls which confirmed that no isotope fractionation was introduced by steps of extraction and reconstitution of samples. An even smaller extent of isotope fractionation of ε = −1.0 ± 0.5‰ was obtained in chemostats at very high dilution D = 0.090 h^{-1} and a high residual substrate concentration of 88 mg L^{-1}. In contrast, in chemostats at D 0.018 h^{-1} with a much lower residual concentration of 90 ± 10 μg L^{-1}, the isotope enrichment factor of 4-CP in chemostats was significantly higher (ε = −4.1 ± 0.2‰, Figure 2B). This value even stands out when comparing it to carbon isotopic enrichment factors reported for biodegradation of other

https://doi.org/10.1021/acs.est.1c04939
Environ. Sci. Technol. 2022, 56, 3021−3032

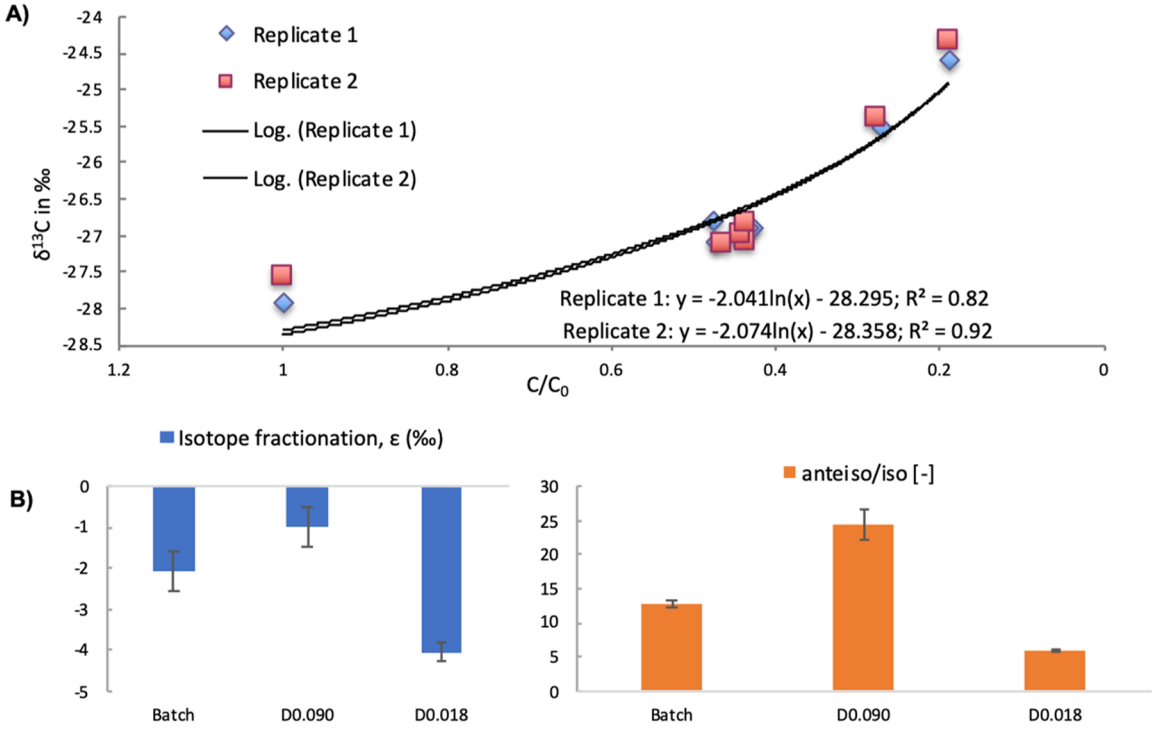

Figure 2. Higher isotope fractionation in chemostat cultivation indicates that 4-CP degradation at low concentrations was not mass transfer-limited. (A) Isotope fractionation (ε) in batch (high concentration data point) was determined according to the Rayleigh equation (eq 4). (B) Isotope fractionation at different dilution points in chemostats. Isotope fractionation in a chemostat was determined by the difference of the isotope values ($\delta^{13}C$) of inflow and outflow (eq 5). Error bars indicate the standard deviation of isotope analysis of samples. A ratio of anteiso vs iso fatty acid shows higher membrane permeability at high concentrations.

phenolic substrates transformed through aromatic ring oxidation such as of phenol ($\varepsilon = -1.5 \pm 0.1‰$),[44] cresol ($\varepsilon = -1.4 \pm 0.2‰$),[44] 2-nitrophenol ($\varepsilon = -1.2 \pm 0.1‰$),[62] 5-methyl-2-nitrophenol ($\varepsilon = -1.3 \pm 0.2‰$),[62] or trichlorinated phenols ($\varepsilon = -0.5$ to $+0.3‰$).[63] The initial step in degradation of 4-CP in *A. chlorophenolicus* A6 is catalyzed by two monooxygenases.[43] Hence, this value may be compared to carbon isotope fractionation in ring monooxygenation from enzyme assays where a possible influence of the cell membrane was eliminated, such as of 2-nitrophenol ($\varepsilon = -1.4 \pm 0.1‰$),[62] 5-methyl-2-nitrophenol ($\varepsilon = -1.5 \pm 0.2‰$),[62] 4-hydroxyphenylacetate ($\varepsilon = -1.1 \pm 0.1‰$),[64] and 4-hydroxybenzoate ($\varepsilon = -0.1 \pm 0.1‰$).[64] Again, these reported values are smaller than the isotope fractionation observed in our study. It is well-recognized and has been demonstrated in an illustrative study by Wijker et al. that intrinsic isotope effects may already be masked on the enzyme level—depending on the presence of "bold" versus "cautious" monooxygenases—so that these values of enzymes and microorganisms likely do not reflect the intrinsic isotope effect of the underlying biochemical reaction.[64] To compare it with tabulated kinetic isotope effects of unmasked reactions, we therefore considered that our observed enrichment factor $\varepsilon = -4.1 \pm 0.2‰$ represents a compound average and that 4-CP contains six carbon atoms so that a position-specific apparent kinetic isotope effect can tentatively be estimated as AKIE = $1/(-0.0041 \cdot 6 + 1) = 1.025$.[65] This value falls toward the upper end of the range of unmasked kinetic isotope effects reported for abiotic C=C bond oxidation (1.011 to 1.024, Table 2 Elsner et al.[65]). We can, therefore, conclude (i) that the degradation of 4-CP at low concentrations was not significantly mass transfer-limited and (ii) that it even represented the intrinsic isotope effect of the underlying biochemical reaction inside the enzyme—otherwise, this intrinsic isotope effect would have been masked.

This increase in isotope fractionation at lower concentrations, however, is in stark contrast with results from our recent study on atrazine degradation, where a dramatic *de*crease in isotope fractionation was observed when substrate concentrations fell below 60 $\mu g\ L^{-1}$.[28] A direct comparison is difficult because—in contrast to atrazine degradation by *A. aurescens* TC1—the regulation of enzyme activity in *A. chlorophenolicus* A6 prevented us from reaching 4-CP concentrations below 85 $\mu g\ L^{-1}$ in our chemostat experiments: when lowering the dilution rate, cell-specific activity also declined so that concentrations remained at the same level, even though a longer residence time was available for degradation. Nonetheless, we observed (i) that the intrinsic isotope effect of the enzyme reaction was strongly expressed at low ($90 \pm 10\ \mu g\ L^{-1}$) concentrations; (ii) that enzyme activity appeared to be strongly regulated under these circumstances; and (iii) that much smaller isotope fractionation was observed at higher concentrations in batch and chemostats. This observation is in contrast to theoretical predictions that smaller isotope fractionation is expected at lower rather than at higher concentrations.[15,16] It therefore highlights a novel type of regulation at low concentrations suggesting either a switch in metabolic pathways and/or that an interplay between changes in membrane permeability and enzyme activity may be at work as hypothesized in the Introduction. In a next step, we therefore considered evidence from the analysis of membrane fatty acids and proteomics to explore a possible role of membrane composition and the regulation of enzyme expression.

https://doi.org/10.1021/acs.est.1c04939
Environ. Sci. Technol. 2022, 56, 3021−3032

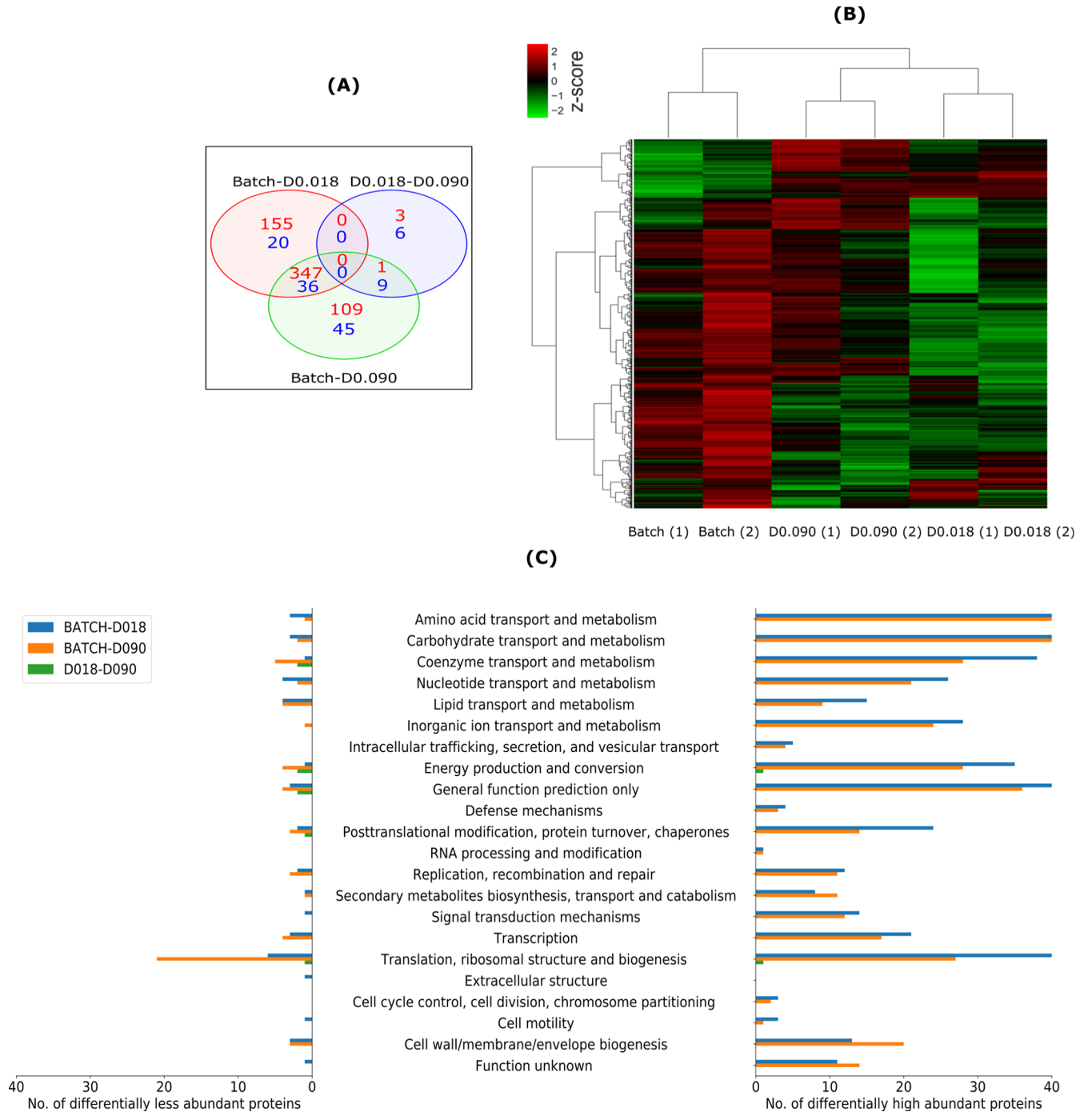

Figure 3. Physiological adaptation at different concentrations in chemostats and batch. (A) Venn diagram illustrates differentially abundant proteins between the three comparison pairs—batch vs chemostat at D0.018 (Batch−D0.018), D0.018 vs chemostat at a dilution rate of 0.090 h^{-1} (D0.018−D0.090), and batch vs D0.090 (Batch−D0.090). Numbers in red represent significantly highly abundant proteins and those in blue represent proteins of significantly low abundance. (B) Heat map representing the clustering of 731 significantly abundant proteins at batch, D0.018, and D0.09. Protein abundance is displayed in the heat map as *z*-scores (i.e., calculated based on how many SD units a protein's abundance is away from the mean abundance derived from all conditions) in the range between 2 (of significantly higher abundance, red) and −2 (of significantly lower abundance, green). Each batch and chemostat cultivation was performed in replicates as indicated by dilution rates in the brackets below the heat map. (C) Distribution of overlapping significantly high- and low-abundant proteins across COG categories in batch, D0.018, and D0.09. First seven COG categories contained proteins for transport and were highly abundant (present at the right side of the tornado plot) in batch compared to D0.018 indicating that the transport of molecules was slow at D0.018.

Fatty Acid Analysis Gives Evidence of Smaller Membrane Permeability at Low Concentrations. The transport across the membrane of bacterial cells is affected by its physical properties, especially by its fatty acid content.[66] The fatty acid content of a cell membrane can change as a result of physiological adaptation.[36,37,40,67] In *A. chlorophenolicus* A6, the predominating fatty acids are iso-pentadecanoic acid (iso-C15:0) and anteiso-pentadecanoic acid (anteiso-C15:0).[5] It is well-established that the ratio of anteiso/iso controls the fluidity or permeability of the membrane, where a

https://doi.org/10.1021/acs.est.1c04939
Environ. Sci. Technol. 2022, 56, 3021−3032

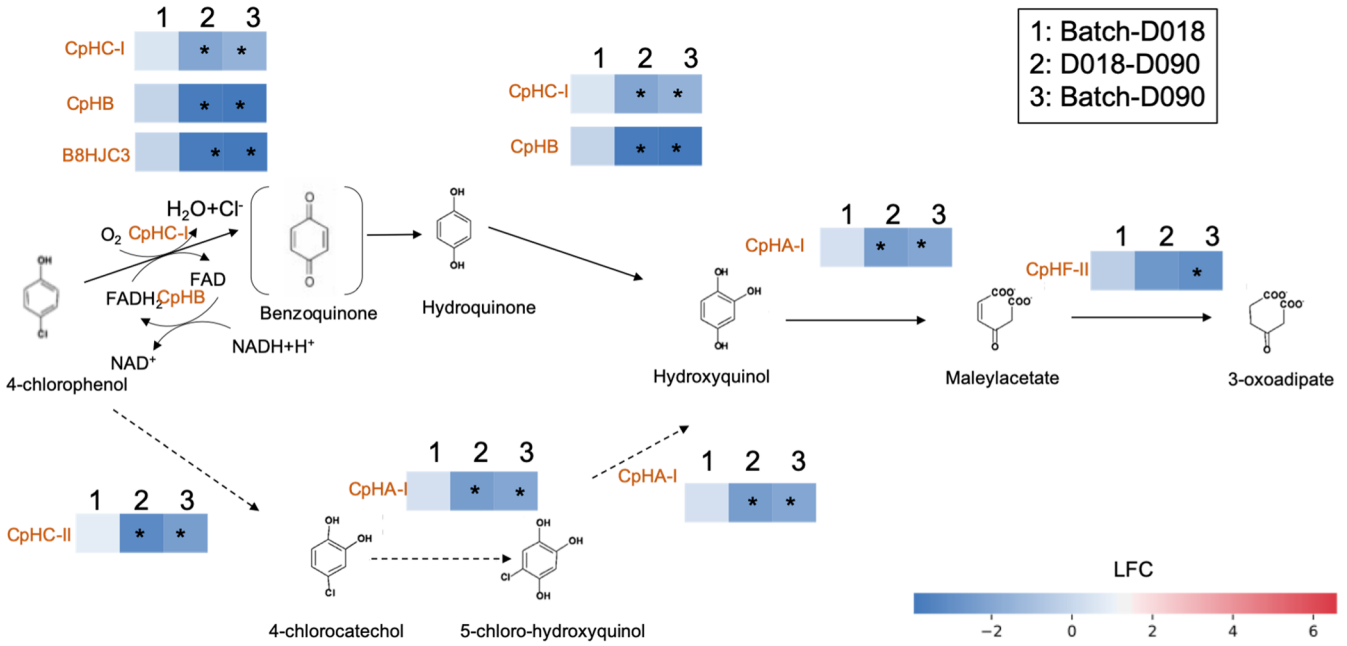

Figure 4. 4-CP degradation pathway adapted from the literature.[43,71,72,77] Three pairwise comparison groups were created as indicated by the numbers 1, 2, and 3. 1: Batch vs chemostat at a dilution rate of 0.018 h^{-1} (Batch-D018). 2: Chemostat at a dilution rate of 0.018 h^{-1} vs chemostat at a dilution rate of 0.090 h^{-1} (D018-D090). 3: Batch vs chemostat at a dilution rate of 0.090 h^{-1} (batch-D090). Different colors represent the LFC in specific proteins from a pairwise comparison between chemostats and batch. Symbols (*) indicate proteins of differential abundance, where the criteria for significant differences were a *P*-value of <0.05 together with a cutoff LFC of $\log_2(2.5)$. The dotted line indicates the postulated pathway, and the brackets indicate the hypothetical intermediate.

high anteiso content makes the membrane more fluid.[37] Surprisingly, measurement of membrane fatty acids showed a greater anteiso-to-iso ratio in batch indicating that the cell membrane was more permeable than at low concentrations in chemostats (Figure 2B). This is contrary to the observation of Unell et al.,[37] where a lower anteiso-to-iso ratio was observed at high 4-CP concentrations—however, under growth on yeast extract with spiked 4-CP so that the results are not directly comparable to our findings. It also contrasts recent findings by Wunderlich et al.[45] who observed that higher 4-CP concentrations resulted in more rigid membranes in *Thaurera aromatica* (higher degree of fatty acid saturation), entailing smaller $^{15}N/^{14}N$ isotope fractionation during nitrate reduction. It is noteworthy that our results represent a specific case where the phenolic compound was used as a growth substrate. We speculate that cells may have abstained from making the membrane rigid so that permeation would not be slowed when an efficient enzyme machinery was in place for catabolic breakdown. Since 4-CP is more lipophilic than nonsubstituted phenols,[37] permeation is likely mediated by diffusion. Nevertheless, to understand the possible role of transporters in the degradation, we looked into the expression of proteins related to transport.

Proteomics Reveals Significantly Lower Abundance of Transport-Related Proteins at Low Concentrations. Microorganisms are known to physiologically adapt to different substrate conditions, for example, by upregulating specific enzymes or transporters, which is generally reflected in the proteome state of the cells.[27−29,68] The proteome state of the cells was analyzed in chemostats at *D* 0.018 and *D* 0.09 and in batch. In total, 1404 proteins were quantified which corresponds to ∼31% coverage of total predicted protein-coding genes in *A. chlorophenolicus* A6 and 1201 proteins were quantified in all the samples (Supporting Information, Table S1). During pairwise comparisons of three cultivation conditions, 731 differentially abundant proteins (either up/downregulated) (Figure 3A) were observed. Hierarchical clustering of differentially abundant proteins shows that many proteins in batch and at D0.09 had a significantly higher abundance (*z*-score around 2) which were less abundant at D0.018 suggesting an adaptation at the cellular level in response to low concentrations (Figure 3B). To perform a functional interpretation, these differentially abundant proteins were linked to clusters of orthologous group categories (COGs)[69] (Figure 3C, Supporting Information, Tables S2−S4). Specific transporters for 4-CP are not known. However, putative transporters which might play a role in 4-CP permeation were highly abundant at high concentrations such as the putative ligand-binding sensor protein (B8H8Y4) (Supporting Information, Tables S2 and S4). This suggests that in the case of transporter-mediated permeation, mass transfer might have been accelerated at high concentrations at batch compared to low concentrations. In this study, therefore, both the fatty acid analysis and proteomics data indicate that the lower isotope fractionation at high concentrations in chemostats is not caused by a less-permeable cell membrane but must have other reasons. In a next step, proteomics was therefore evaluated to explore regulation on the level of enzyme expression.

Differential Expression of Proteins Related to 4-CP Degrading Enzymes at Low Concentrations. As discussed above, the high isotope fractionation ($\varepsilon = -4.1 \pm 0.2‰$) in chemostats (D0.018) gives unequivocal evidence that enzymatic turnover was slow relative to mass transfer at low concentrations—otherwise, intrinsic isotope effects would not have been so strongly expressed. When interpreting this value in comparison with the lower observable isotope fractionation at high concentrations in batch and chemostats at D0.09, the

https://doi.org/10.1021/acs.est.1c04939
Environ. Sci. Technol. 2022, 56, 3021−3032

decisive step is the enzyme reaction of the initial irreversible transformation. Compared to atrazine transformation by *A. aurescens* TC1, 4-CP transformation by *A. chlorophenolicus* A6 is more complex because it may involve two possible initial pathways,[43] which are encoded by a chlorophenol degradation (cph) gene cluster involving different proteins (Figure 4, Supporting Information, Table S5). One initial oxidative degradation pathway of 4-CP is catalyzed by CphCI and CphB which—together with flavin reductase (B8HJC3)—form a two-component flavin-diffusible monooxygenase (TC-FDM).[43,70−72] CphB reduces FAD to $FADH_2$ via NADH, whereas CphCI uses $FADH_2$ to activate molecular O_2 for oxidation of 4-CP to hydroxyquinone.[71,72] The second degradation pathway is catalyzed by the CphCII protein which has been postulated to oxidize 4-CP to 4-chlorocatechol.[43] Here, the degradation mechanism has not been elucidated yet. Consequently, the turnover of 4-CP can be the result of two parallel transformations catalyzed by CphCI and CphCII, and the observable isotope fractionation may be the weighted average of both, where it would mostly reflect the predominant pathway. The observation that breakdown by different enzymes causes different isotope effects in organic pollutants has been made previously for dioxygenases in nitroaromatic compound oxidation[73] or for ring versus methyl group oxidation of toluene[74]

Hence, when interpreting the smaller value of ε at high concentrations in batch in comparison with the large ε in chemostats at D0.018, the modulated ε may either be evidence of masked isotope fractionation due to mass transfer or the result of a metabolic shift between the two initial pathways of Figure 4 leading to a different weighted average of isotope effects from two different enzymes. In this case, one would expect regulation of one enzymatic pathway *relative* to the other at high versus low concentrations (CphCI vs CphCII).

Direct observation of either pathway was not possible because our chemical analysis was not optimized to measure the respective short-lived intermediates (hydroxyquinone vs 4-chlorocatechol). However, to understand the regulation on the degradation of 4-CP at low concentrations, proteins related to the 4-CP degradation pathway could be compared between D0.018, D0.09, and batch (Figure 4). We observed that CphCI and CphCII were both differentially less abundant at D0.018 compared to D0.090 (Supporting Information, Table S5, Figure 4). This indicates that downregulation of enzymes is a possible reason for the higher isotope fractionation observed at low concentrations. Alternatively, a shift in degradation pathways might play a role. Indeed, abundance of CphCI was fourfold reduced, whereas CphCII was eightfold less abundant (Supporting Information, Table S5). Both CphCI and CphCII are inducible not constitutive,[42] and evidence from previous work suggests that both pathways were co-occurring at high concentrations (no kinetic preference).[43] Hence, the expression level of CphCI and CphCII might also contribute to a dominance of one degradation pathway. In this study, the relative abundance of CphCI was higher than CphCII under all conditions. However, a small shift in the ratio of CphCI/CphCII—about half from D018 (202:1) and batch (159:1) to D090 (90:1)—was observed (Supporting Information, Table S5), which might also produce a small shift in degradation pathways. Hence, our analysis highlights physiological adaptation on the enzyme expression level—both with respect to total abundance of catabolic enzymes (CphCI and CphCII) and with respect to a possible shift in metabolic pathways (CphCI and CphCII) at low concentrations.

This total abundance (CphCI and CphCII) also explains the observed regulation on 4-CP turnover in chemostats, which decreased with lower dilution rates leading to the same residual substrate concentration at different dilution rates, Figure 1, and the situation that two different q_s were observed at the same residual concentrations (0.66 ± 0.12 vs 1.54 ± 0.65 mg S mg C_x^{-1} h^{-1} at D of 0.018 and 0.038 h^{-1}, respectively, See Supporting Information, Table S6). At high D (0.09), a high q_s (6.14 ± 0.88 mg S^{-1} mg C_x h^{-1}) was observed indicating that degradation became faster at high concentrations and became smaller at low concentrations in chemostats, consistent with our conclusions about enzyme activity regulation at low concentrations mentioned above. Specifically, when the feeding pump was stopped, only very slow degradation was observed over 60 min in chemostats at a residual (=effluent) concentration of 90 ± 5 μg L^{-1} (Supporting Information, Figure S5). This is in contrast to atrazine degradation, where we observed rapid degradation of atrazine in chemostats at a residual (=effluent) concentration of 60 μg L^{-1}.[28] Besides the downregulation of proteins (Figure 3), the overall reduced metabolism was also reflected in the morphology of cells (Supporting Information, Figure S4).

Environmental Significance. In natural oligotrophic environments such as groundwater, heterotrophic bacteria feed on a multitude of naturally occurring organic compounds that have in common that they occur only in small concentrations. Hence, understanding bacterial regulation and adaptation under such low-energy conditions is of general importance—as much for the persistence of organic matter in carbon budgeting, as for bioremediation of low-level chemical pollution. To explore possible underlying patterns of adaptation, this study has focused on degradation of one substrate (4-CP) by one strain in a setup of deliberately reduced complexity. Even though this experimental design does not directly mimic natural groundwater conditions, it has the advantage that it enables a relevant generic process understanding by allowing us to combine evidence from CSIA, membrane fatty acid analysis, and the analysis of the proteome state of the cells. This multidisciplinary approach revealed (i) that the enzymatic turnover inside bacteria of the studied strain *A. chlorophenolicus* A6 was regulated at multiple levels at low concentrations (μg L^{-1}) including membrane composition, as well as differential expression of enzymes and/or a possible shift in metabolic pathways, and (ii) that this regulation resulted in a situation that substrate supply through the cell membrane did not become rate-limiting at low concentrations but that rather enzyme activity inside the cell was down-regulated first. Since this observation is in stark contrast to the observation of mass transfer limitation in low-level atrazine degradation by *A. aurescens* TC1[28] or of 2,6-dichlorobenzamide degradation by *Aminobacter* sp. MSH1,[75] the present study reveals a different pattern of microbial adaptation to low concentrations: bacteria downregulated their enzymatic activity instead of running into limited substrate supply. Hence, the pattern observed here reveals another "end-member behavior" on the scale of physiological adaptation of degrading bacteria that can be expected in low-energy environments. Remarkably, this physiological limitation was observed at a concentration around 90 μg L^{-1}. Considering that $\Delta_R G0'$cat = −111 ± 5 kJ·mol^{-1} and that the observed specific substrate consumption rate observed was 0.66 mg S g

https://doi.org/10.1021/acs.est.1c04939
Environ. Sci. Technol. 2022, 56, 3021−3032

$C_x^{-1}\cdot h^{-1}$, this concentration is much higher than the minimum substrate concentration required for maintenance of cells' viability.[76] Cells can physiologically adapt under extremely low energy fluxes which will enable moving to much lower concentrations with a near-zero growth rate.[27] Nonetheless, in this study, degradation was observed to become slow already at 90 $\mu g\ L^{-1}$ indicating that microbial adaptation by enzyme regulation would curb bioremediation efforts—or utilization of organic matter—at low concentrations. Based on this insight, we conclude that bioaugmentation approaches would seem most promising when they rely on bacteria that maintain their intrinsic enzyme activity high so that they run into mass transfer limitations as an ultimate physical limit before downregulating their metabolism. The discovery of such specific physiological adaptation in degrading bacteria emphasizes the need for a knowledge base for management of bioremediation of different pollutants that account for bacterial adaptation. In future studies, it will, hence, be important to study degradation of other contaminants by different microorganisms to better understand limitations of mass transfer versus enzymatic turnover on micropollutant degradation—or organic substrates in general—at low concentrations and design strategies to overcome them.

■ ASSOCIATED CONTENT

Supporting Information

The Supporting Information is available free of charge at https://pubs.acs.org/doi/10.1021/acs.est.1c04939.

Materials and methods; HPLC method for 4-CP concentration measurement; estimation of growth kinetic parameters; EA-IRMS measurement for determination of reference values; method for analysis of the carbon isotope in 4-CP samples; lipid extraction and membrane fatty acid analysis; proteomics analysis; schematic diagram of the custom-made bioreactor used in this study; degradation of 4-CP and cell concentration in a batch cultivation experiment; observed specific growth rate at different residual 4-CP concentrations in batch; degradation profile of 4-CP at 95 μg L-1 shows slow enzymatic turnover; change in morphology at different dilution points in chemostats and batch; NMDS of all conditions used for proteomics analysis; heat map representing the clustering of quantified proteins; Voom transformation of the proteomics data; GC-IRMS chromatogram of low-concentration extracts; proteomics data analysis; and biomass and yield measured at different dilution rates after achieving steady states in chemostats (PDF)

■ AUTHOR INFORMATION

Corresponding Authors

Kankana Kundu − *Institute of Groundwater Ecology, Helmholtz Zentrum Munchen, 85764 Neuherberg, Bavaria, Germany; Center for Microbial Ecology and Technology (CMET), Faculty of Bioscience Engineering, University of Ghent, 9000 Ghent, Belgium;* orcid.org/0000-0001-7147-157X; Email: kankanakundu@gmail.com

Martin Elsner − *Institute of Groundwater Ecology, Helmholtz Zentrum Munchen, 85764 Neuherberg, Bavaria, Germany; Chair of Analytical Chemistry and Water Chemistry, Technical University of Munich, D-85748 Garching, Germany;* orcid.org/0000-0003-4746-9052; Phone: +49 89 2180-78232; Email: m.elsner@tum.de

Authors

Aileen Melsbach − *Institute of Groundwater Ecology, Helmholtz Zentrum Munchen, 85764 Neuherberg, Bavaria, Germany; Chair of Analytical Chemistry and Water Chemistry, Technical University of Munich, D-85748 Garching, Germany*

Benjamin Heckel − *Institute of Groundwater Ecology, Helmholtz Zentrum Munchen, 85764 Neuherberg, Bavaria, Germany*

Sarah Schneidemann − *Institute of Groundwater Ecology, Helmholtz Zentrum Munchen, 85764 Neuherberg, Bavaria, Germany*

Dheeraj Kanapathi − *Institute of Groundwater Ecology, Helmholtz Zentrum Munchen, 85764 Neuherberg, Bavaria, Germany*

Sviatlana Marozava − *Institute of Groundwater Ecology, Helmholtz Zentrum Munchen, 85764 Neuherberg, Bavaria, Germany*

Juliane Merl-Pham − *Core Facility Proteomics, Helmholtz Zentrum München, 80939 Munich, Germany*

Complete contact information is available at: https://pubs.acs.org/10.1021/acs.est.1c04939

Author Contributions

The manuscript was written through contributions of all authors. All authors have given approval to the final version of the manuscript.

Notes

The authors declare no competing financial interest.

■ ACKNOWLEDGMENTS

This work was funded by an ERC consolidator grant ("MicroDegrade", grant no. 616861) awarded by the European Research Council.

■ REFERENCES

(1) Fenner, K.; Canonica, S.; Wackett, L. P.; Elsner, M. Evaluating Pesticide Degradation in the Environment: Blind Spots and Emerging Opportunities. *Science* **2013**, *341*, 752−758.

(2) Shannon, M. A.; Bohn, P. W.; Elimelech, M.; Georgiadis, J. G.; Mariñas, B. J.; Mayes, A. M. Science and Technology for Water Purification in the Coming Decades. *Nature* **2008**, *452*, 301−310.

(3) Shao, Y.; Chen, Z.; Hollert, H.; Zhou, S.; Deutschmann, B.; Seiler, T.-B. Toxicity of 10 Organic Micropollutants and Their Mixture: Implications for Aquatic Risk Assessment. *Sci. Total Environ.* **2019**, *666*, 1273−1282.

(4) Strong, L. C.; Rosendahl, C.; Johnson, G.; Sadowsky, M. J.; Wackett, L. P. Arthrobacter aurescens TC1 Metabolizes Diverse s -Triazine Ring Compounds. 2002, *68* (12), 5973−5980 DOI: 10.1128/aem.68.12.5973-5980.2002

(5) Westerberg, K.; Elväng, A. M.; Stackebrandt, E.; Jansson, J. K. Arthrobacter Chlorophenolicus Sp. Nov., a New Species Capable of Degrading High Concentrations of 4-Chlorophenol. *Int. J. Syst. Evol. Microbiol.* **2000**, *50*, 2083−2092.

(6) Kolvenbach, B. A.; Helbling, D. E.; Kohler, H.-P. E.; Corvini, P. F.-X. Emerging Chemicals and the Evolution of Biodegradation Capacities and Pathways in Bacteria. *Curr. Opin. Biotechnol.* **2014**, *27*, 8−14.

(7) Arrieta, J. M.; Mayol, E.; Hansman, R. L.; Herndl, G. J.; Dittmar, T.; Duarte, C. M. Dilution Limits Dissolved Organic Carbon Utilization in the Deep Ocean. *Science* **2015**, *348*, 331−333.

(8) Hofmann, R.; Griebler, C. DOM and Bacterial Growth Efficiency in Oligotrophic Groundwater: Absence of Priming and Co-Limitation by Organic Carbon and Phosphorus. *Aquat. Microb. Ecol.* **2018**, *81*, 55−71.
(9) Egli, T. How to Live at Very Low Substrate Concentration. *Water Res.* **2010**, *44*, 4826−4837.
(10) Griebler, C.; Mindl, B.; Slezak, D. Combining DAPI and SYBR Green II for the Enumeration of Total Bacterial Numbers in Aquatic Sediments. *Int. Rev. Hydrobiol.* **2001**, *86*, 453−465.
(11) Whitman, W. B.; Coleman, D. C.; Wiebe, W. J. Prokaryotes: The Unseen Majority. *Proc. Natl. Acad. Sci. U.S.A.* **1998**, *95*, 6578−6583.
(12) Tabor, P. S.; Neihof, R. A. Improved Microautoradiographic Method to Determine Individual Microorganisms Active in Substrate Uptake in Natural Waters. *Appl. Environ. Microbiol.* **1982**, *44*, 945−953.
(13) Teira, E.; Reinthaler, T.; Pernthaler, A.; Pernthaler, J.; Herndl, G. J. Combining Catalyzed Reporter Deposition-Fluorescence in Situ Hybridization and Microautoradiography to Detect Substrate Utilization by Bacteria and Archaea in the Deep Ocean. *Appl. Environ. Microbiol.* **2004**, *70*, 4411−4414.
(14) Bosma, T. N. P.; Middeldorp, P. J. M.; Schraa, G.; Zehnder, A. J. B. Mass Transfer Limitation of Biotransformation: Quantifying Bioavailability. *Environ. Sci. Technol.* **1996**, *31*, 248−252.
(15) Thullner, M.; Kampara, M.; Richnow, H. H.; Harms, H.; Wick, L. Y. Impact of Bioavailability Restrictions on Microbially Induced Stable Isotope Fractionation. 1. Theoretical Calculation. *Environ. Sci. Technol.* **2008**, *42*, 6544−6551.
(16) Kampara, M.; Thullner, M.; Richnow, H. H.; Harms, H.; Wick, L. Y. Impact of Bioavailability Restrictions on Microbially Induced Stable Isotope Fractionation. 2. Experimental Evidence. *Environ. Sci. Technol.* **2008**, *42*, 6552−6558.
(17) Heijnen, J. J. Bioenergetics of Microbial Growth. *Encyclopedia of Industrial Biotechnology: Bioprocess, Bioseparation, and Cell Technology*; Wiley Online Library, 1999.
(18) Trautwein, K.; Lahme, S.; Wöhlbrand, L.; Feenders, C.; Mangelsdorf, K.; Harder, J.; Steinbüchel, A.; Blasius, B.; Reinhardt, R.; Rabus, R. Physiological and Proteomic Adaptation of "Aromatoleum Aromaticum"EbN1 to Low Growth Rates in Benzoate-Limited, Anoxic Chemostats. *J. Bacteriol.* **2012**, *194*, 2165−2180.
(19) Melander, L. C. S.; Saunders, W. H. *Reaction Rates of Isotopic Molecules*; John Wiley & Sons, 1980.
(20) Meyer, A. H.; Penning, H.; Elsner, M. C and N Isotope Fractionation Suggests Similar Mechanisms of Microbial Atrazine Transformation despite Involvement of Different Enzymes (AtzA and TrzN). *Environ. Sci. Technol.* **2009**, *43*, 8079−8085.
(21) Ehrl, B. N.; Gharasoo, M.; Elsner, M. Isotope Fractionation Pinpoints Membrane Permeability as a Barrier to Atrazine Biodegradation in Gram-Negative Polaromonas Sp. Nea-C. *Environ. Sci. Technol.* **2018**, *52*, 4137−4144.
(22) O'Leary, M. H. Carbon Isotopes in Photosynthesis. *Bioscience* **1988**, *38*, 328−336.
(23) Wilkes, E. B.; Carter, S. J.; Pearson, A. CO2-Dependent Carbon Isotope Fractionation in the Dinoflagellate Alexandrium Tamarense. *Geochim. Cosmochim. Acta* **2017**, *212*, 48−61.
(24) Laws, E. A.; Popp, B. N.; Bidigare, R. R.; Kennicutt, M. C.; Macko, S. A. Dependence of Phytoplankton Carbon Isotopic Composition on Growth Rate and [CO2) Aq: Theoretical Considerations and Experimental Results. *Geochim. Cosmochim. Acta* **1995**, *59*, 1131−1138.
(25) Aeppli, C.; Berg, M.; Cirpka, O. A.; Holliger, C.; Schwarzenbach, R. P.; Hofstetter, T. B. Influence of Mass-Transfer Limitations on Carbon Isotope Fractionation during Microbial Dechlorination of Trichloroethene. *Environ. Sci. Technol.* **2009**, *43*, 8813−8820.
(26) Vonberg, D.; Vanderborght, J.; Cremer, N.; Pütz, T.; Herbst, M.; Vereecken, H. 20 Years of Long-Term Atrazine Monitoring in a Shallow Aquifer in Western Germany. *Water Res.* **2014**, *50*, 294−306.
(27) Kundu, K.; Marozava, S.; Ehrl, B.; Merl-Pham, J.; Griebler, C.; Elsner, M. Defining Lower Limits of Biodegradation: Atrazine Degradation Regulated by Mass Transfer and Maintenance Demand in Arthrobacter Aurescens TC1. *ISME J.* **2019**, *13*, 2236−2251.
(28) Ehrl, B. N.; Kundu, K.; Gharasoo, M.; Marozava, S.; Elsner, M. Rate-Limiting Mass Transfer in Micropollutant Degradation Revealed by Isotope Fractionation in Chemostat. *Environ. Sci. Technol.* **2019**, *53*, 1197−1205.
(29) Marozava, S.; Röling, W. F. M.; Seifert, J.; Küffner, R.; Von Bergen, M.; Meckenstock, R. U. Physiology of Geobacter Metallireducens under Excess and Limitation of Electron Donors. Part II. Mimicking Environmental Conditions during Cultivation in Retentostats. *Syst. Appl. Microbiol.* **2014**, *37*, 287−295.
(30) Trautwein, K.; Grundmann, O.; Wöhlbrand, L.; Eberlein, C.; Boll, M.; Rabus, R. Benzoate Mediates Repression of C4-Dicarboxylate Utilization in "Aromatoleum Aromaticum" EbN1. *J. Bacteriol.* **2012**, *194*, 518−528.
(31) Edwards, V. H. The Influence of High Substrate Concentrations on Microbial Kinetics. *Biotechnol. Bioeng.* **1970**, *12*, 679−712.
(32) Haldane, J. B. S. *Enzymes*; MIT Press: Cambridge, 1965.
(33) Hao, O. J.; Kim, M. H.; Seagren, E. A.; Kim, H. Kinetics of Phenol and Chlorophenol Utilization by Acinetobacter Species. *Chemosphere* **2002**, *46*, 797−807.
(34) DiMarco, A. A.; Averhoff, B.; Ornston, L. N. Identification of the Transcriptional Activator PobR and Characterization of Its Role in the Expression of PobA, the Structural Gene for p-Hydroxybenzoate Hydroxylase in Acinetobacter Calcoaceticus. *J. Bacteriol.* **1993**, *175*, 4499−4506.
(35) Egli, T. The Ecological and Physiological Significance of the Growth of Heterotrophic Microorganisms with Mixtures of Substrates. *Advances in Microbial Ecology*; Springer, 1995; pp 305−386.
(36) Heipieper, H. J.; Meinhardt, F.; Segura, A. The Cis–Trans Isomerase of Unsaturated Fatty Acids in Pseudomonas and Vibrio: Biochemistry, Molecular Biology and Physiological Function of a Unique Stress Adaptive Mechanism. *FEMS Microbiol. Lett.* **2003**, *229*, 1−7.
(37) Unell, M.; Kabelitz, N.; Jansson, J. K.; Heipieper, H. J. Adaptation of the Psychrotroph Arthrobacter Chlorophenolicus A6 to Growth Temperature and the Presence of Phenols by Changes in the Anteiso/Iso Ratio of Branched Fatty Acids. *FEMS Microbiol. Lett.* **2007**, *266*, 138−143.
(38) Jensen, J. Chlorophenols in the Terrestrial Environment. *Reviews of Environmental Contamination and Toxicology*; Springer, 1996; pp 25−51.
(39) Wild, S.; Harrad, S. J.; Jones, K. C. Chlorophenols in Digested UK Sewage Sludges. *Water Res.* **1993**, *27*, 1527−1534.
(40) Weber, F. J.; de Bont, J. A. M. Adaptation Mechanisms of Microorganisms to the Toxic Effects of Organic Solvents on Membranes. *Biochim. Biophys. Acta, Rev. Biomembr.* **1996**, *1286*, 225−245.
(41) Basak, B.; Bhunia, B.; Dutta, S.; Dey, A. Enhanced Biodegradation of 4-Chlorophenol by Candida Tropicalis PHB5 via Optimization of Physicochemical Parameters Using Taguchi Orthogonal Array Approach. *Int. Biodeterior. Biodegrad.* **2013**, *78*, 17−23.
(42) Scheublin, T. R.; Deusch, S.; Moreno-Forero, S. K.; Müller, J. A.; van der Meer, J. R.; Leveau, J. H. J. Transcriptional Profiling of G Ram-Positive A Rthrobacter in the Phyllosphere: Induction of Pollutant Degradation Genes by Natural Plant Phenolic Compounds. *Environ. Microbiol.* **2014**, *16*, 2212−2225.
(43) Nordin, K.; Unell, M.; Jansson, J. K. Novel 4-Chlorophenol Degradation Gene Cluster and Degradation Route via Hydroxyquinol in Arthrobacter Chlorophenolicus A6. *Appl. Environ. Microbiol.* **2005**, *71*, 6538−6544.
(44) Wei, X.; Gilevska, T.; Wetzig, F.; Dorer, C.; Richnow, H.-H.; Vogt, C. Characterization of Phenol and Cresol Biodegradation by Compound-Specific Stable Isotope Analysis. *Environ. Pollut.* **2016**, *210*, 166−173.

https://doi.org/10.1021/acs.est.1c04939
Environ. Sci. Technol. 2022, 56, 3021−3032

(45) Wunderlich, A.; Heipieper, H. J.; Elsner, M.; Einsiedl, F. Solvent Stress-Induced Changes in Membrane Fatty Acid Composition of Denitrifying Bacteria Reduce the Extent of Nitrogen Stable Isotope Fractionation during Denitrification. *Geochim. Cosmochim. Acta* **2018**, *239*, 275−283.
(46) Props, R.; Monsieurs, P.; Vandamme, P.; Leys, N.; Denef, V. J.; Boon, N. Gene Expansion and Positive Selection as Bacterial Adaptations to Oligotrophic Conditions. *Msphere* **2019**, *4*, No. e00011.
(47) Pfennig, N.; Wagener, S. An Improved Method of Preparing Wet Mounts for Photomicrographs of Microorganisms. *J. Microbiol. Methods* **1986**, *4*, 303−306.
(48) Hoefs, J.; Hoefs, J. *Stable Isotope Geochemistry*; Springer, 2009; Vol. *285*.
(49) Coplen, T. B. Guidelines and Recommended Terms for Expression of Stable-Isotope-Ratio and Gas-Ratio Measurement Results. *Rapid Commun. Mass Spectrom.* **2011**, *25*, 2538−2560.
(50) Hayes, J. M. Practice and Principles of Isotopic Measurements in Organic Geochemistry. *Org. Geochem. Contemp. Anc. Sediments* **1983**, *5*, No. e5.
(51) Werner, R. A.; Brand, W. A. Referencing Strategies and Techniques in Stable Isotope Ratio Analysis. *Rapid Commun. Mass Spectrom.* **2001**, *15*, 501−519.
(52) Sherlock. Microbial Identification System, *MIS Operating Manual*, 2012, pp 2.7−2.18.
(53) Wiśniewski, J. R.; Zougman, A.; Nagaraj, N.; Mann, M. Universal Sample Preparation Method for Proteome Analysis. *Nat. Methods* **2009**, *6*, 359−362.
(54) Ritchie, M. E.; Phipson, B.; Wu, D.; Hu, Y.; Law, C. W.; Shi, W.; Smyth, G. K. Limma Powers Differential Expression Analyses for RNA-Sequencing and Microarray Studies. *Nucleic Acids Res.* **2015**, *43*, No. e47.
(55) Law, C. W.; Chen, Y.; Shi, W.; Smyth, G. K. Voom: Precision Weights Unlock Linear Model Analysis Tools for RNA-Seq Read Counts. *Genome Biol.* **2014**, *15*, R29.
(56) Smyth, G. K. Linear Models and Empirical Bayes Methods for Assessing Differential Expression in Microarray Experiments. *Stat. Appl. Genet. Mol. Biol.* **2004**, *3*, 1−25.
(57) Benjamini, Y.; Hochberg, Y. Controlling the False Discovery Rate: A Practical and Powerful Approach to Multiple Testing. *J. R. Stat. Soc., Ser. B* **1995**, *57*, 289−300.
(58) Waskom, M.; Botvinnik, O.; O'Kane, D.; Hobson, P.; David, Y. H.; Lukauskas, S.; Cole, J. B.; Warmenhoven, J.; de Ruiter, J.; Hoyer, S.; et al. *Seaborn*: V0. 9.0; Zenodo, 2018; Vol. *10*.
(59) Reed, M. C.; Lieb, A.; Nijhout, H. F. The Biological Significance of Substrate Inhibition: A Mechanism with Diverse Functions. *Bioessays* **2010**, *32*, 422−429.
(60) Bakhshi, Z.; Najafpour, G.; Kariminezhad, E.; Pishgar, R.; Mousavi, N.; Taghizade, T. Growth Kinetic Models for Phenol Biodegradation in a Batch Culture of Pseudomonas Putida. *Environ. Technol.* **2011**, *32*, 1835−1841.
(61) Ereqat, S. I.; Abdelkader, A. A.; Nasereddin, A. F.; Al-Jawabreh, A. O.; Zaid, T. M.; Letnik, I.; Abdeen, Z. A. Isolation and Characterization of Phenol Degrading Bacterium Strain Bacillus Thuringiensis J20 from Olive Waste in Palestine. *J. Environ. Sci. Health, Part A: Toxic/Hazard. Subst. Environ. Eng.* **2018**, *53*, 39−45.
(62) Wijker, R. S.; Zeyer, J.; Hofstetter, T. B. Isotope Fractionation Associated with the Simultaneous Biodegradation of Multiple Nitrophenol Isomers by Pseudomonas Putida B2. *Environ. Sci.: Processes Impacts* **2017**, *19*, 775−784.
(63) Bernstein, A.; Golan, R.; Gelman, F.; Kuder, T. Microbial Oxidation of Tri-Halogenated Phenols-Multi-Element Isotope Fractionation. *Int. Biodeterior. Biodegrad.* **2019**, *145*, 104811.
(64) Wijker, R. S.; Pati, S. G.; Zeyer, J.; Hofstetter, T. B. Enzyme Kinetics of Different Types of Flavin-Dependent Monooxygenases Determine the Observable Contaminant Stable Isotope Fractionation. *Environ. Sci. Technol. Lett.* **2015**, *2*, 329−334.
(65) Elsner, M.; Zwank, L.; Hunkeler, D.; Schwarzenbach, R. P. A New Concept Linking Observable Stable Isotope Fractionation to Transformation Pathways of Organic Pollutants. *Environ. Sci. Technol.* **2005**, *39*, 6896−6916.
(66) Kaneda, T. Iso-and Anteiso-Fatty Acids in Bacteria: Biosynthesis, Function, and Taxonomic Significance. *Microbiol. Mol. Biol. Rev.* **1991**, *55*, 288−302.
(67) Sinensky, M. Homeoviscous Adaptation—a Homeostatic Process That Regulates the Viscosity of Membrane Lipids in Escherichia Coli. *Proc. Natl. Acad. Sci. U.S.A.* **1974**, *71*, 522−525.
(68) Marozava, S.; Vargas-López, R.; Tian, Y.; Merl-Pham, J.; Braster, M.; Meckenstock, R. U.; Smidt, H.; Röling, W. F. M.; Westerhoff, H. V. Metabolic Flexibility of a Prospective Bioremediator: Desulfitobacterium Hafniense Y51 Challenged in Chemostats. *Environ. Microbiol.* **2018**, *20*, 2652−2669.
(69) Tatusov, R. L.; Galperin, M. Y.; Natale, D. A.; Koonin, E. V. The COG Database: A Tool for Genome-Scale Analysis of Protein Functions and Evolution. *Nucleic Acids Res.* **2000**, *28*, 33−36.
(70) Arora, P.; Bae, H. Bacterial Degradation of Chlorophenols and Their Derivatives. *Microb. Cell Fact.* **2014**, *13*, 31.
(71) Kang, C.; Yang, J. W.; Cho, W.; Kwak, S.; Park, S.; Lim, Y.; Choe, J. W.; Kim, H. S. Oxidative Biodegradation of 4-Chlorophenol by Using Recombinant Monooxygenase Cloned and Overexpressed from Arthrobacter Chlorophenolicus A6. *Bioresour. Technol.* **2017**, *240*, 123−129.
(72) Cho, S. Y.; Kwean, O. S.; Yang, J. W.; Cho, W.; Kwak, S.; Park, S.; Lim, Y.; Kim, H. S. Identification of the Upstream 4-Chlorophenol Biodegradation Pathway Using a Recombinant Monooxygenase from Arthrobacter Chlorophenolicus A6. *Bioresour. Technol.* **2017**, *245*, 1800−1807.
(73) Pati, S. G.; Kohler, H.-P. E.; Pabis, A.; Paneth, P.; Parales, R. E.; Hofstetter, T. B. Substrate and Enzyme Specificity of the Kinetic Isotope Effects Associated with the Dioxygenation of Nitroaromatic Contaminants. *Environ. Sci. Technol.* **2016**, *50*, 6708−6716.
(74) Dorer, C.; Vogt, C.; Kleinsteuber, S.; Stams, A. J. M.; Richnow, H.-H. Compound-Specific Isotope Analysis as a Tool to Characterize Biodegradation of Ethylbenzene. *Environ. Sci. Technol.* **2014**, *48*, 9122−9132.
(75) Sun, F.; Mellage, A.; Gharasoo, M.; Melsbach, A.; Cao, X.; Zimmermann, R.; Griebler, C.; Thullner, M.; Cirpka, O. A.; Elsner, M. Mass-Transfer-Limited Biodegradation at Low Concentrations—Evidence from Reactive Transport Modeling of Isotope Profiles in a Bench-Scale Aquifer. *Environ. Sci. Technol.* **2021**, *55*, 7385.
(76) Tijhuis, L.; Van Loosdrecht, M. C. M.; Heijnen, J. J. A Thermodynamically Based Correlation for Maintenance Gibbs Energy Requirements in Aerobic and Anaerobic Chemotrophic Growth. *Biotechnol. Bioeng.* **1993**, *42*, 509−519.
(77) Suma, Y.; Lim, H.; Kwean, O. S.; Cho, S.; Yang, J.; Kim, Y.; Kang, C. S.; Kim, H. S. Enzymatic Degradation of Aromatic Hydrocarbon Intermediates Using a Recombinant Dioxygenase Immobilized onto Surfactant-Activated Carbon Nanotube. *Bioresour. Technol.* **2016**, *210*, 117−122.

https://doi.org/10.1021/acs.est.1c04939
Environ. Sci. Technol. 2022, 56, 3021−3032